Supporting Information

Visualizing RNA conformational changes via Pattern Recognition of RNA by Small Molecules

Christopher S. Eubanks[a], Bo Zhao[b], Neeraj N. Patwardhan[a], Rhese D. Thompson[b], Qi Zhang[b] and Amanda E. Hargrove[a]

a) Department of Chemistry, Duke University, Durham, NC 27708, United States.

b) Department Biochemistry and Biophysics, University of North Carolina, Chapel Hill, Chapel Hill, NC 27599-7260, United States.

Corresponding Author
* E-mail: amanda.hargrove@duke.edu; Tel.: 919-660-1522

Contents

S1. Riboswitch Principal Component Analysis

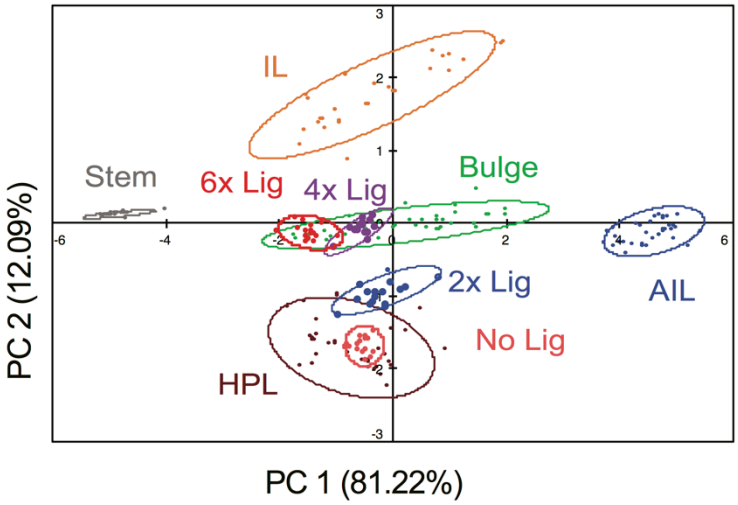

Figure S1-1. PCA plot of PreQ1 ligand concentration relative to PreQ1-RS. Ligand was added at 2x (400 nM), 4x (800 nM), and 6x (1.2 μM) and are shown above. Additionally, ligand concentration from 2 – 4 μM were found to have excessive background fluorescence from the ligand (greater than 20% of the total fluorescence) and were not able to be used in the assay. The assay was run in the following conditions (10 mM NaH_2PO_4, 25 mM NaCl, 4 mM $MgCl_2$, 0.5 mM EDTA, pH 7.3, heated to 25°C) at 322 nm excitation and 455 nm emission.

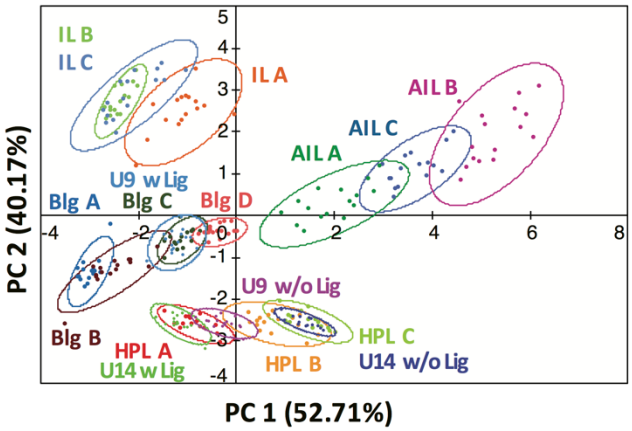

Figure S1-2. PCA plot of PreQ1 U9 and U14 RNA constructs within individual motif assay conditions (10 mM NaH_2PO_4, 25 mM NaCl, 4 mM $MgCl_2$, 0.5 mM EDTA, 8 mM PEG 12,000, pH 7.3, heated to 37°C). The clustering predicts the correct secondary structure identity and nucleotide sizes for unbound and bound states of the RNA constructs.

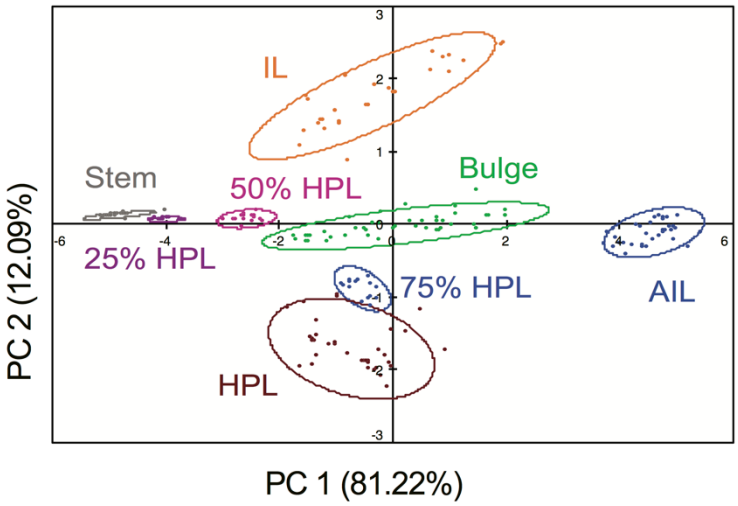

Figure S1-3. PCA plot of ratio of stem A and HP A for determining the differences in clustering for multiple RNA structures. RNA concentration was held at 200 nM with 75:25, 50:50, and 25:75 HP:Stem ratios. The assay was run in the following conditions (10 mM NaH_2PO_4, 25 mM NaCl, 4 mM $MgCl_2$, 0.5 mM EDTA, pH 7.3, heated to 25°C) at 322 nm excitation and 455 nm emission.

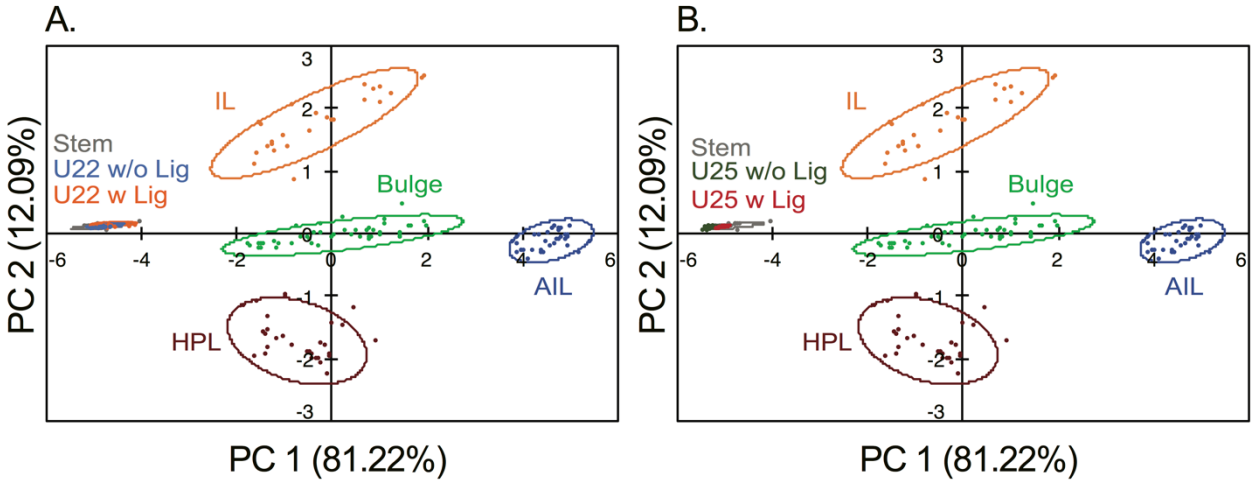

Figure S1-4. A. PCA plot of PreQ1-BFU-U22 with and without PreQ1 ligand which are both predicted to be stem structures. B. PCA plot of F-RS-BFU-U25 with and without fluoride ligand which are both predicted to be stem structures. Both assays were run in Condition A (10 mM NaH_2PO_4, 25 mM NaCl, 4 mM $MgCl_2$, 0.5 mM EDTA, pH 7.3, heated to 25°C)

S2. NMR titration of Fluoride and PreQ1 Riboswitches

Samples prepared for NMR spectroscopy were initially exchanged to water, and subsequently exchanged to 10 mM sodium phosphate (pH 6.4), 50 mM KCl, and 50 μM EDTA. All NMR spectra were collected on a Bruker Avance III 500 and 600 spectrometer equipped with 5 mm triple-resonance QCI and TCI cryogenic probes, respectively. ^{1}H NMR imino proton spectra were recorded in H_2O at 10°C and 30°C. Magnesium chloride was titrated directly into the NMR samples of the BFU fluoride riboswitches in ratios to RNA indicated in the corresponding figure. Upon addition of magnesium to saturating conditions (5 mM) at the final magnesium titration point, sodium fluoride was titrated into the same sample at the ratios indicated in the corresponding figure. Pre-queuosine$_1$ was added directly into the NMR samples of BFU modified preQ1-I riboswitches to the ratios indicated in the corresponding figure. Note that since the known K_{sp} for the equilibrium [Mg^{2+} + $2F^{-}$ ⇆ MgF_2] is 6.4 ×10^{-3} mM, there is no precipitation expected at the high working concentrations of 5 mM $MgCl_2$ and 10 mM NaF. Moreover, even at higher RNA concentrations required for NMR studies (0.1 mM) the riboswitch can be expected to be saturated at these salt concentrations.

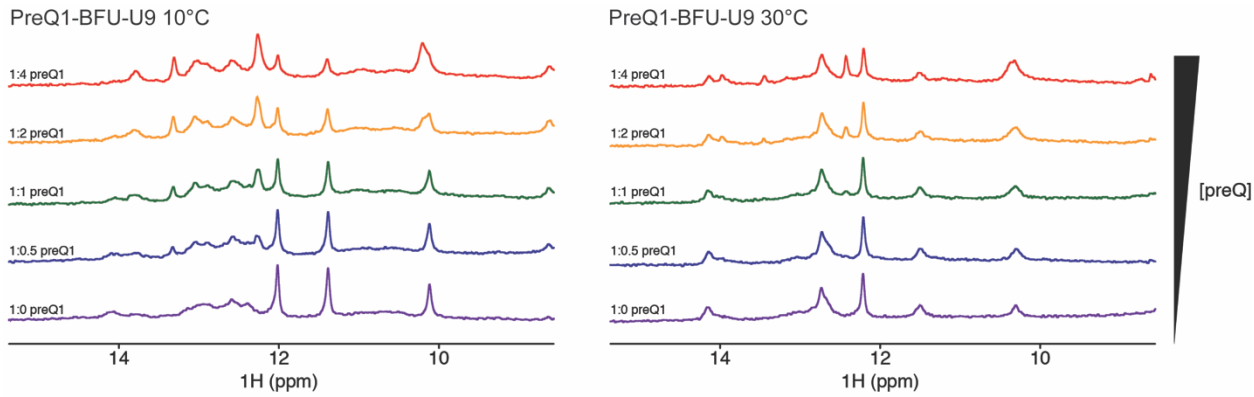

Figure S2-1. NMR titration of BFU U9 modified Preq1 riboswitch. Titration of PreQ1 (0, 50, 100, 200, and 400 μM) was performed Addition of Preq1 ligand showed binding to the riboswitch at both 10 or 30°C.

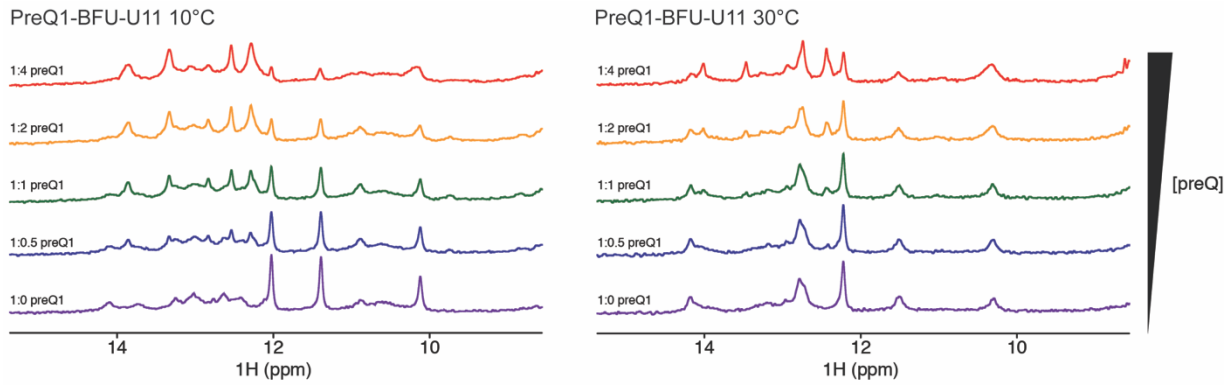

Figure S2-2. NMR titration of BFU U11 modified Preq1 riboswitch. Titration of PreQ1 (0, 50, 100, 200, and 400 μM) was performed Addition of Preq1 ligand showed binding to the riboswitch at both 10 or 30°C.

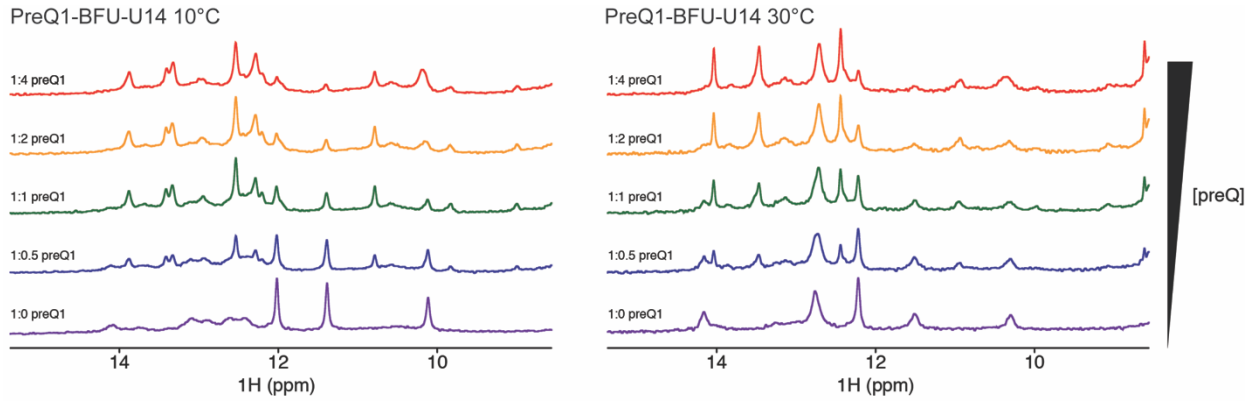

Figure S2-3. NMR titration of BFU U14 modified Preq1 riboswitch. Titration of PreQ1 (0, 50, 100, 200, and 400 μM) was performed Addition of Preq1 ligand showed binding to the riboswitch at both 10 or 30°C.

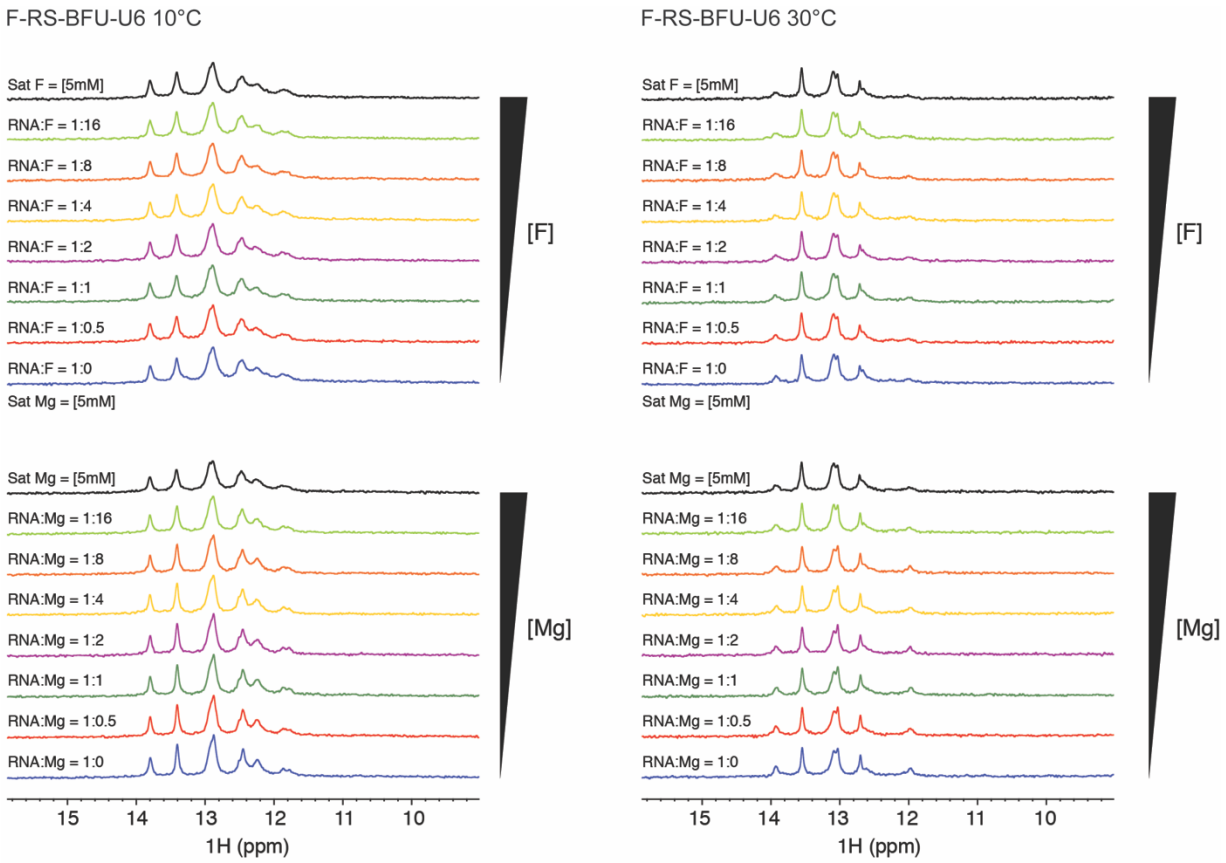

Figure S2-4. NMR titration of BFU U6 modified fluoride riboswitch. Titration of magnesium (0, 50, 100, 200, 400, 800, 1600, and 5000 μM) was performed first, followed by addition of fluoride (same titration concentrations as magnesium. Addition of magnesium and fluoride did not show any change in the NMR peaks, suggesting no binding of magnesium or fluoride by the BFU U6 fluoride riboswitch at either 10 or 30°C.

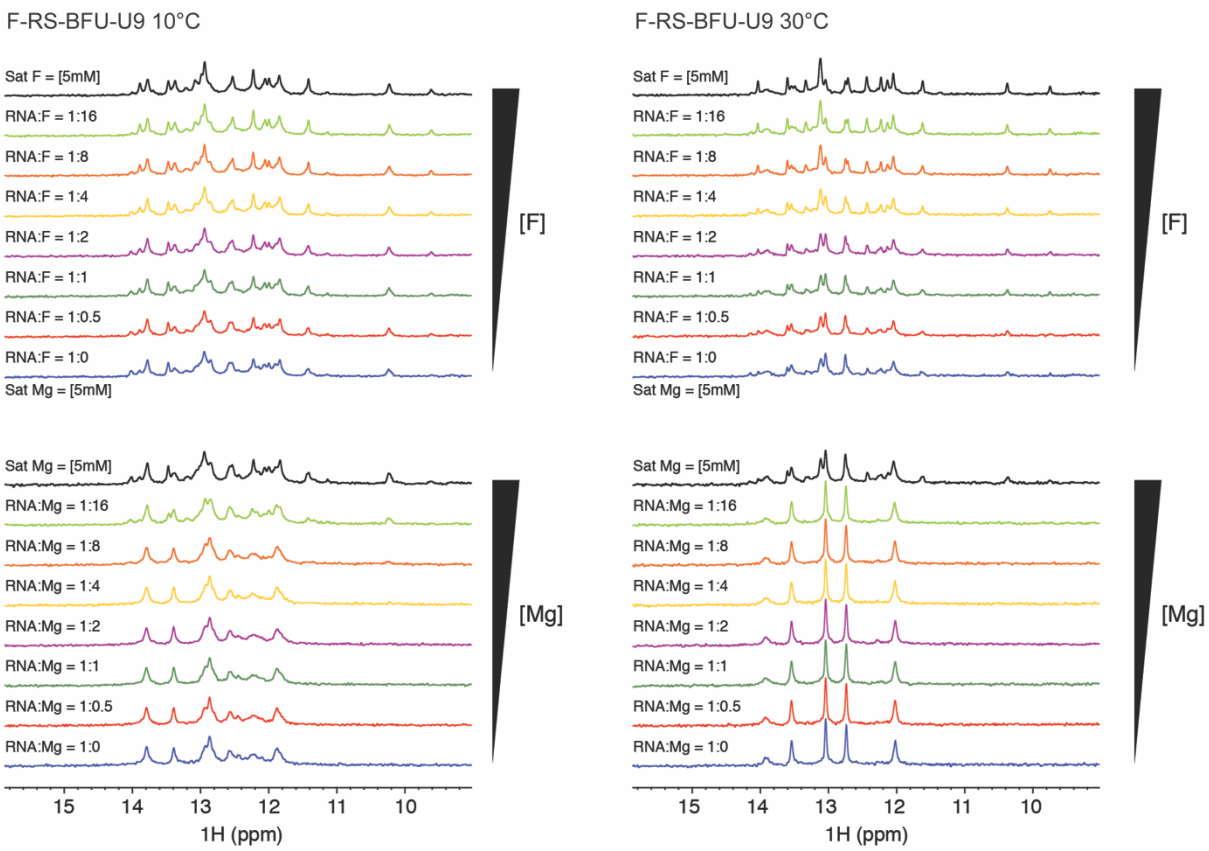

Figure S2-5. NMR titration of BFU U9 modified fluoride riboswitch. Titration of magnesium (0, 50, 100, 200, 400, 800, 1600, and 5000 μM) was performed first, followed by addition of fluoride (same titration concentrations as magnesium. The RNA construct showed weak magnesium binding at 10°C and slightly enhanced binding at 30°C. Upon addition of fluoride, the construct bound fluoride at both temperatures, but was comparatively weaker binder than wild-type fluoride riboswitch.

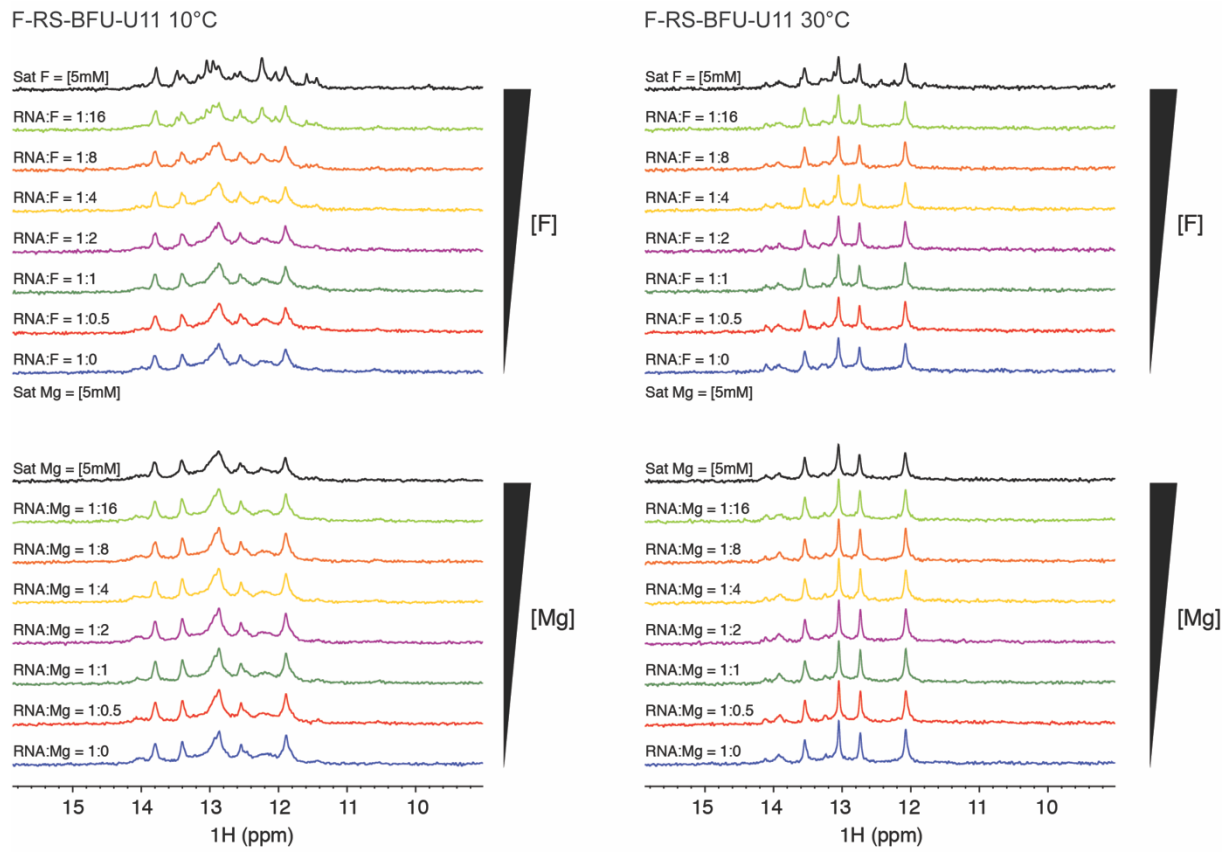

Figure S2-6. NMR titration of BFU U11 modified fluoride riboswitch. Titration of magnesium (0, 50, 100, 200, 400, 800, 1600, and 5000 μM) was performed first, followed by addition of fluoride (same titration concentrations as magnesium. Addition of magnesium showed no changes in the NMR peaks at either temperature, and only showed weak binding to fluoride at 10°C.

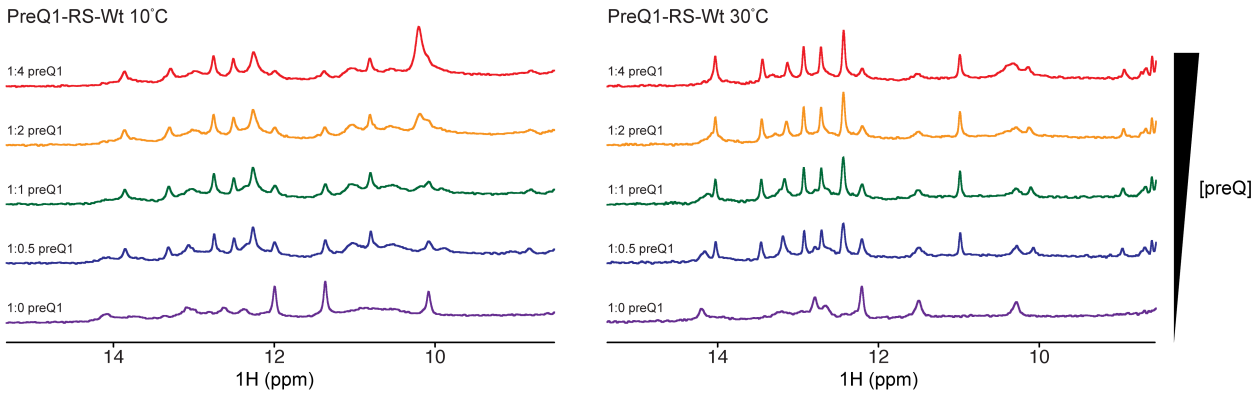

Figure S2-7. NMR titration of unmodified Preq1 riboswitch. Titration of PreQ1 (0, 30, 60, 120, and 240 μM) was performed in 60 μM Preq1 riboswitch sample. Addition of Preq1 ligand showed binding to the riboswitch at both 10 and 30°C.

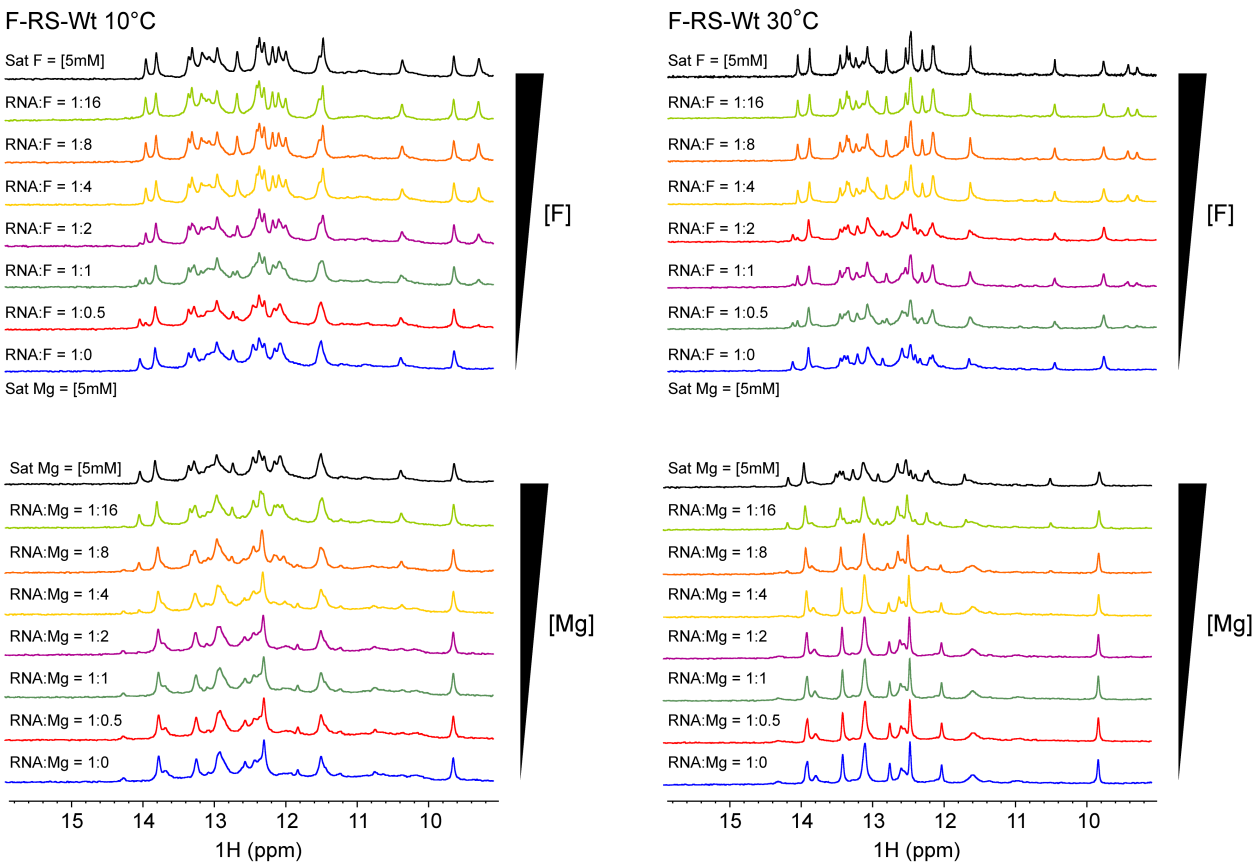

Figure S2-8. NMR titration of unmodified fluoride riboswitch. Titration of magnesium (0, 50, 100, 200, 400, 800, 1600, and 5000 μM) was performed first, followed by addition of fluoride (same titration concentrations as magnesium). Addition of magnesium and fluoride showed binding to the riboswitch at both 10 and 30°C.

S3. RNA Solid Phase Synthesis and Purification

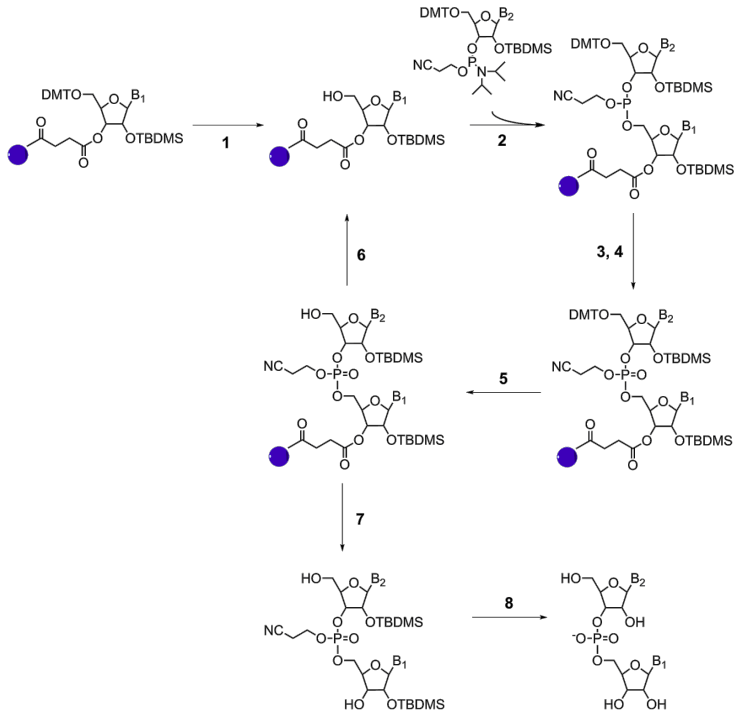

Scheme S3-1. Outline of solid phase synthesis cycle. Key: 1. Detritylation; 2. Activation and Coupling; 3. Capping; 4. Oxidation, I_2; 5. Detritylation; 6. Next cycle; 7. Cleavage from solid-phase; 8. Deprotections.

A solid phase synthesizer was used for synthesis of all RNA sequences and allowed for selective modification with the BFU nucleoside. Three fluoride riboswitch constructs (BFU modified at U6, U9, and U11) and three PreQ1 constructs (BFU modified at U9, U11, and U14) were synthesized. Orthogonally protected adenosine, guanosine, cytosine, uracil, and BFU phosphoramidite were dissolved in anhydrous acetonitrile. Polystyrene columns were used with the first 3' nucleotide attached. For each nucleotide, the 4,4' dimethoxytrityl group was removed with trichloroacetic acid. The next nucleotide was incorporated using a tetrazole catalyst. Unreacted 5' hydroxyl groups are capped with acetic anhydride and N-methylimidazole dissolved in tetrahydrofuran/pyridine. Finally, the phosphodiester bond is oxidized with iodine in pyridine/water mixture, which increases the stability of the RNA sequence. The synthesis is then repeated until the RNA sequence has been fully synthesized.

Purification of the RNA sequences began with cleavage of the RNA off the solid phase support and deprotection of the bases of the sequences with 333 µL x3 ammonium methylamine for 7.5 minutes and then allowed to incubate for two hours. Afterwards, the solutions were dried down using a vacuum concentrator until crystals were formed. To deprotect the 2' hydroxyl group, crystals were dissolved in 115 µL dimethyl sulfoxide, 60 µL triethylamine, and 75 µL of triethylamine: hydrogen fluoride (30%) and heated for 2 ½ hours at 65 °C. After cooling to room temperature, 1.75 mL of quenching buffer (Glen Research) is added to the solutions. Finally, a polydivinylbenzene 4,4' dimethoxytrityl affinity column was used to purify the RNA sequence. The columns are pre-conditioned with 0.5 mL acetonitrile and 1 mL 2M triethylammonium acetate (TEAA). The RNA sequence solutions are added to the column, washed with 1 mL of a 1:9 acetonitrile:TEAA solution, 1 mL water, 2 mL trifluoroacetic acid, and 2 mL water. Subsequently the RNA is eluted from the column, and the 4,4' dimethoxytrityl group is removed, with 1 mL of 1M ammonium bicarbonate. The RNA is ethanol precipitated and is lyophilized to remove any remaining ethanol. The RNA sequences were dissolved in phosphate buffer (10 mM NaH_2PO_4, 25 mM NaCl, 4 mM $MgCl_2$, 0.5 mM EDTA, pH 7.3), and the concentration was analyzed using a Nanodrop spectrophotometer. The purity of the RNA was determined with pre-cast 15% polyacrylamide gel electrophoresis (PAGE) run with 1X tris, borate, and EDTA (TBE) buffer. The gels were run with sample at 180 V for ~2 hours. Afterwards, the gel was stained with Diamond dye® for 30 minutes.

S4. Materials and Methods

All reactions were performed under a nitrogen atmosphere passed through drierite absorbents (Fisher Scientific), unless otherwise indicated. Reagents and anhydrous solvents (excluding CH_2Cl_2) were purchased from Glen Research, Sigma-Aldrich, Acros, Fisher, ChemImpex, and Oakwood Chemicals and were used as received without further purification. Anhydrous CH_2Cl_2 was obtained using a Pure Solv (Innovative Technology) solvent purification system at Duke

University. The benzofuranyl uridine synthesis reactions were performed based on previous literature conditions.[1] Deionized water was obtained from an ELGA PURELAB Flex (Veolia Water Technologies) water purification system. Diethylpyrocarbonate (DEPC) treated water was used for RNAse free solutions. Water was treated with DEPC (1% v/v) overnight to remove all RNAse, and was subsequently autoclaved at 120°C for 30 minutes to decompose the unreacted DEPC. Plate reader assays were run on a SpectraMax I3 (Molecular Devices) and used Corning 4514 384 well plates. The assays were run based on previous literature conditions.[1] Polyethylene glycol (PEG) 12,000 was purchased from Alfa Aesar and used without further purification. The design and analysis of the RNA training set and its effect in both buffer conditions utilized was explored in previous literature.[1-2]

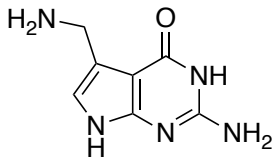

Pre-Q1

2-amino-5-(aminomethyl)-3,7-dihydro-4*H*-pyrrolo[2,3-*d*] pyrimidin-4-one (PreQ1): Synthesized using a reported synthetic pathway.[3] Characterization data for final product PreQ-1 provided below: ^{1}H NMR (400 MHz, CD_3OD) δ 6.81 (s, 1H), 4.16 (s, 2H); ^{13}C NMR (126 MHz, DMSO-d_6) δ 160.2, 152.7, 152.2, 116.2, 110.4, 98.3, 35.5. HRMS (ESI+): Calculated for $C_7H_{10}N_5O^+$ [M+H]: 180.0880, Found: 180.0880 (± 0.1 ppm). HPLC analysis (Performed on a Phenomex-C_{18} reverse phase column using water (with 0.1% v/v of TFA) and acetonitrile (Gradient - 90:10 to 10:90) as eluents): Ret. time – 2.305 min, Purity – 99%

^{1}H-NMR (400 MHz, CD_3OD): for PreQ1

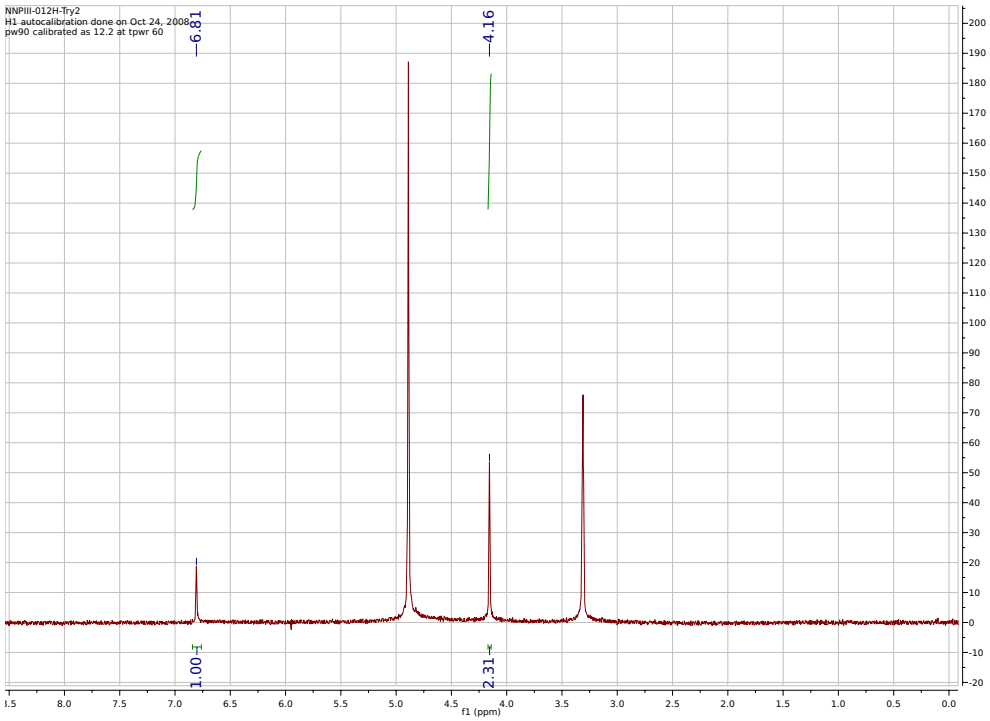

^{13}C-NMR (125 MHz, DMSO-d_6): for PreQ1

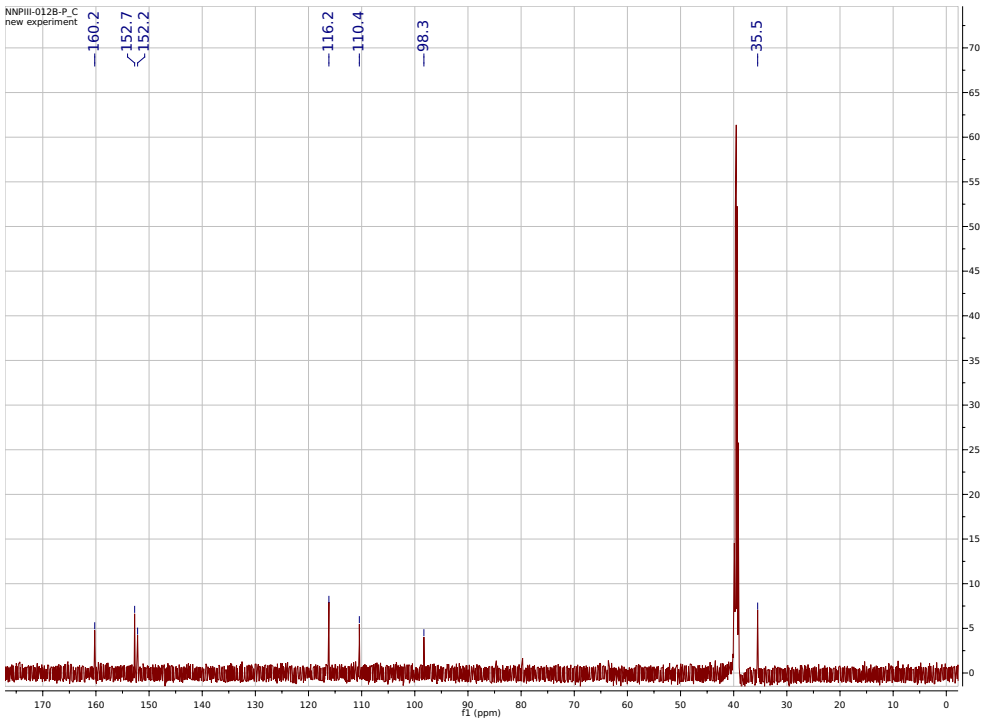

HPLC Analysis of PreQ1:

SHIMADZU LabSolutions

Analysis Report

<Sample Information>

Sample Name	: NNPIII-012BRepurifR4		
Sample ID	: NNPIII-012BRepurifR4		
Data Filename	: NNPIII-012BRepurifR4.lcd		
Method Filename	: NNP-Grd10-90_Slow_PDA_D2only.lcm		
Batch Filename	: NNP_04_09_2018.lcb		
Vial #	: 1-100	Sample Type	: Unknown
Injection Volume	: 5 uL		
Date Acquired	: 4/10/2018 10:14:38 AM	Acquired by	: chemist
Date Processed	: 4/10/2018 10:37:44 AM	Processed by	: chemist

<Chromatogram>

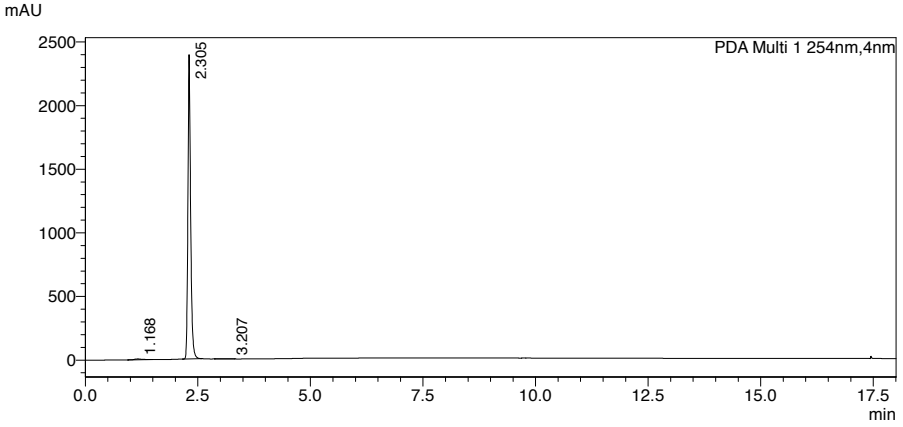

<Peak Table>

PDA Ch1 254nm

Peak#	Ret. Time	Area	Area%
1	1.168	75261	0.745
2	2.305	10006882	99.026
3	3.207	23120	0.229
Total		10105263	100.000

S5. Aminoglycoside Receptor: Riboswitch Titration Graphs

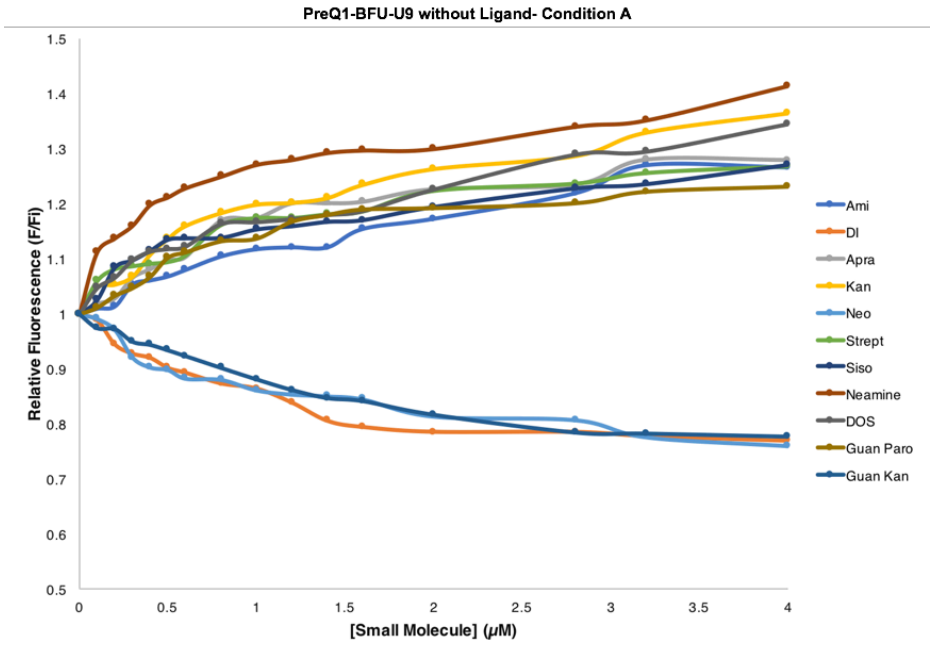

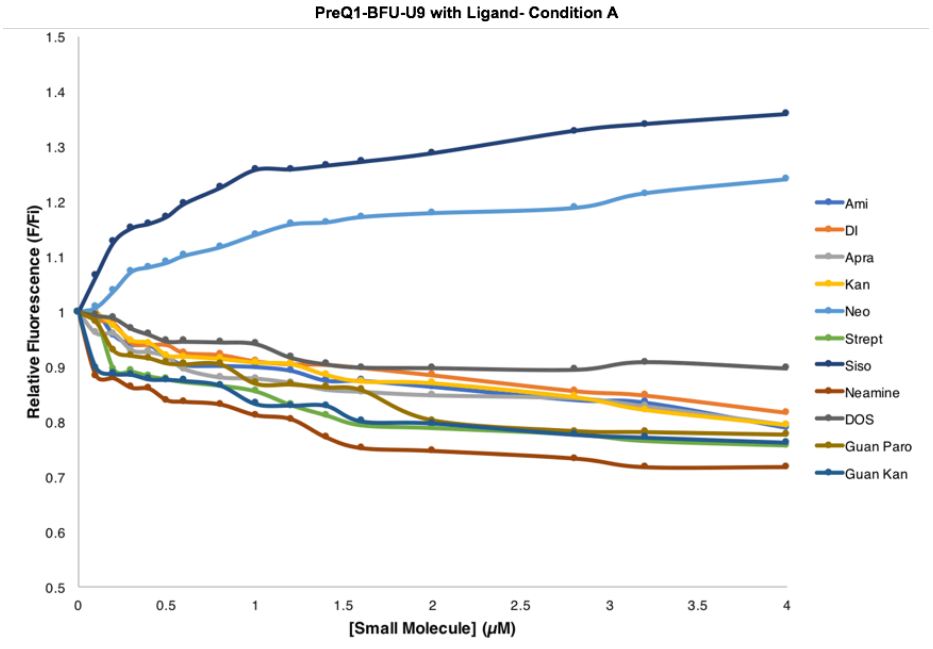

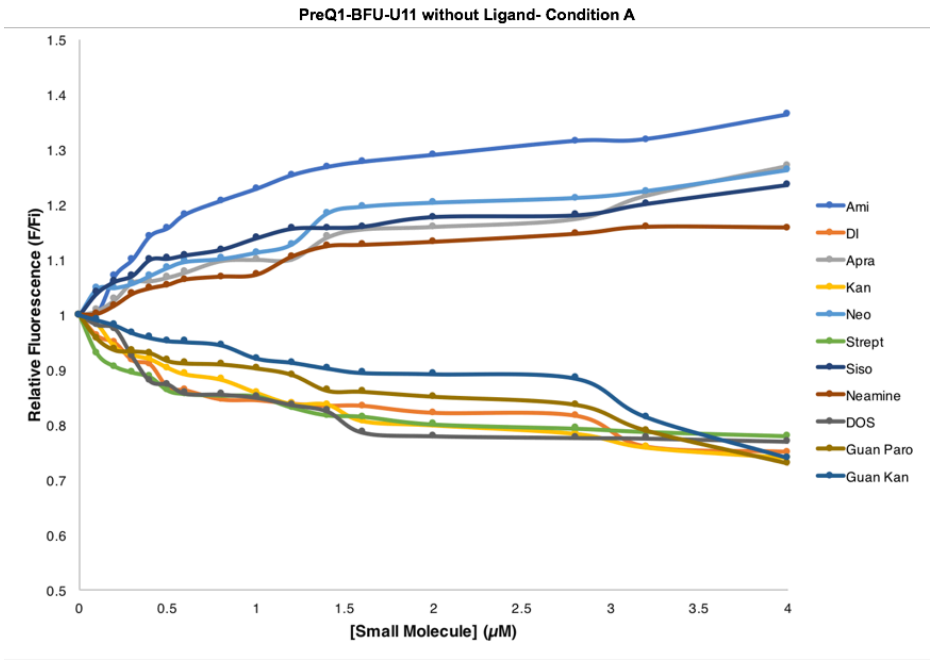
PreQ1-BFU-U11 without Ligand- Condition A
Relative Fluorescence (F/Fi)
[Small Molecule] (μM)
Ami
Dl
Apra
Kan
Neo
Strept
Siso
Neamine
DOS
Guan Paro
Guan Kan

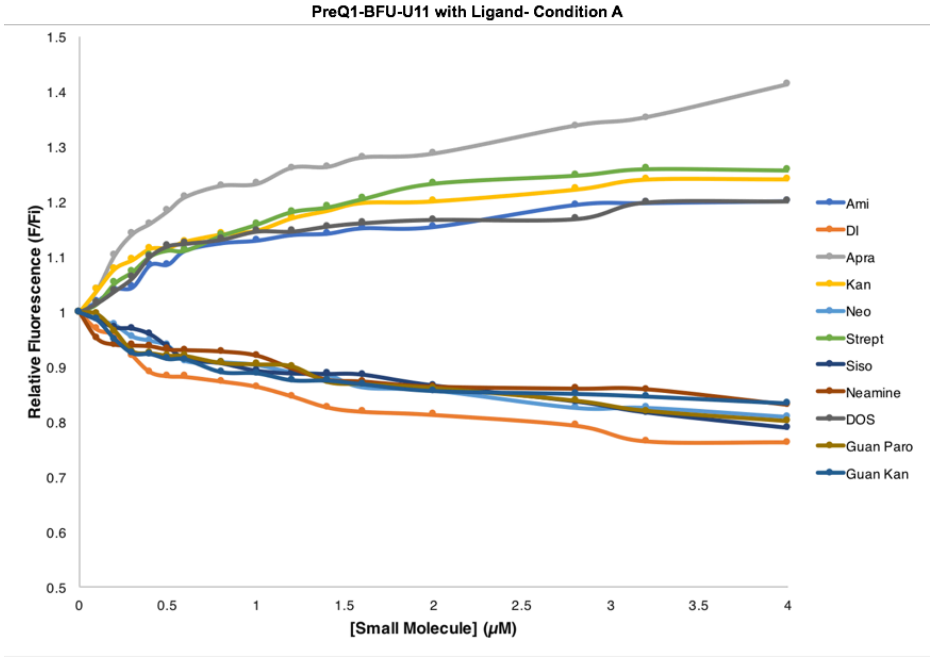
PreQ1-BFU-U11 with Ligand- Condition A
Relative Fluorescence (F/Fi)
[Small Molecule] (μM)
Ami
Dl
Apra
Kan
Neo
Strept
Siso
Neamine
DOS
Guan Paro
Guan Kan

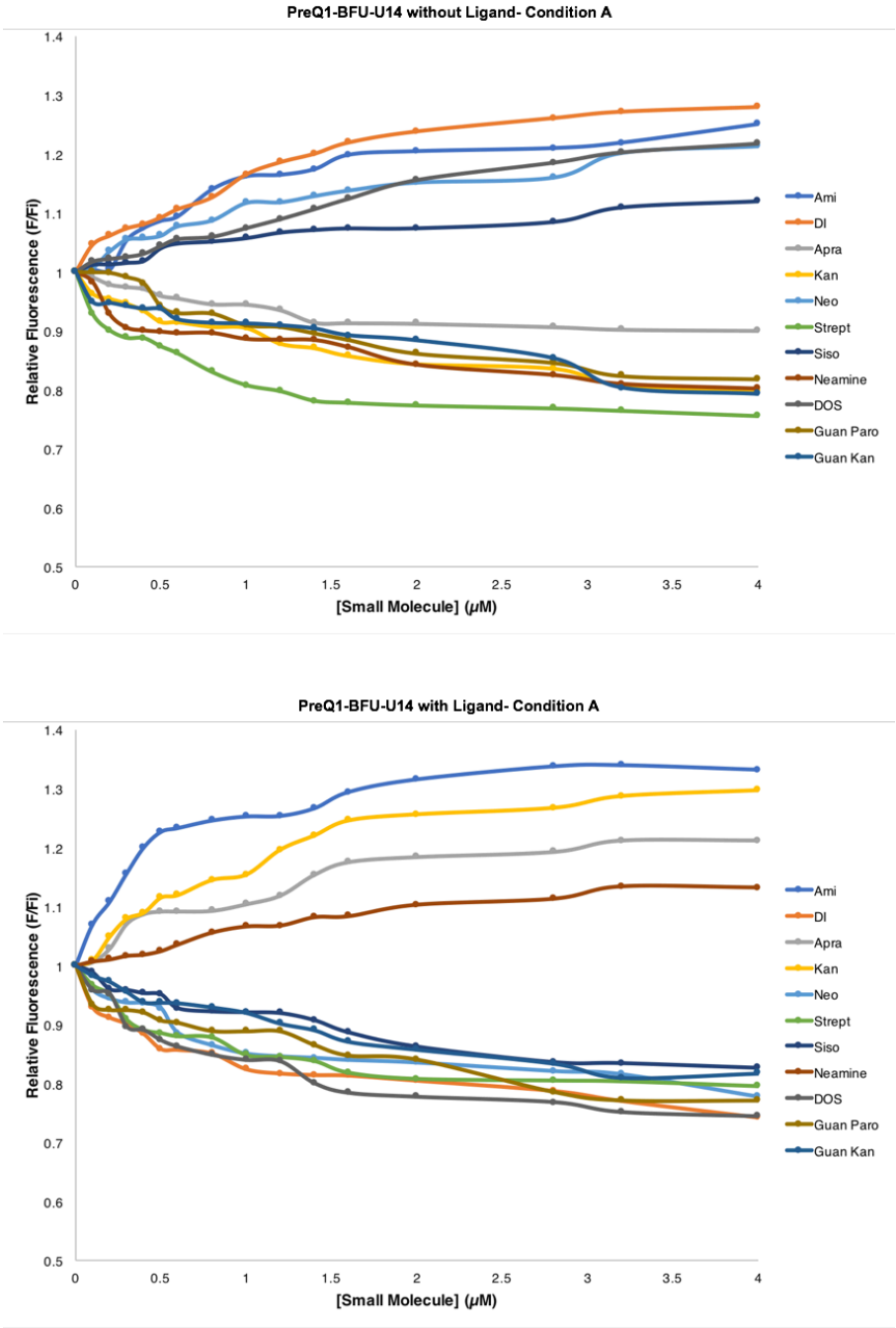

Figure S5-1. PreQ1 riboswitch RNA constructs titration curves to the small molecule receptors in a standard buffer (10 mM NaH_2PO_4, 25 mM NaCl, 4 mM $MgCl_2$, 0.5 mM EDTA, pH 7.4) in the absence or presence of ligand (1.2 μM PreQ1). Each graph shows a single RNA sequence and the receptors titration curves. The error for all experiments were less than 10%. The error was calculated using the standard error of triplicates, and relative standard error was determined based on the mean of each RNA sequence.

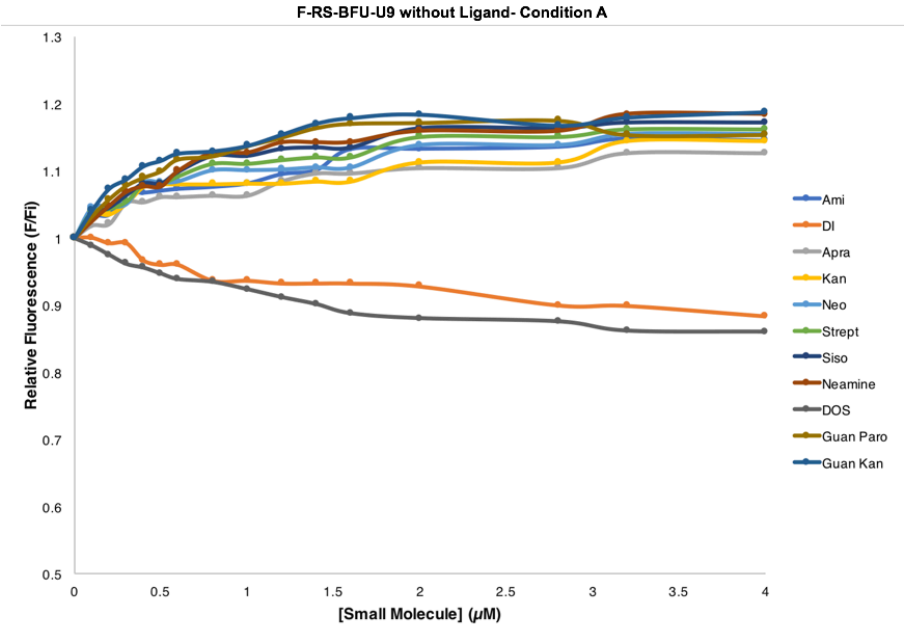
F-RS-BFU-U9 without Ligand- Condition A
Relative Fluorescence (F/Fi)
[Small Molecule] (μM)
Ami
DI
Apra
Kan
Neo
Strept
Siso
Neamine
DOS
Guan Paro
Guan Kan

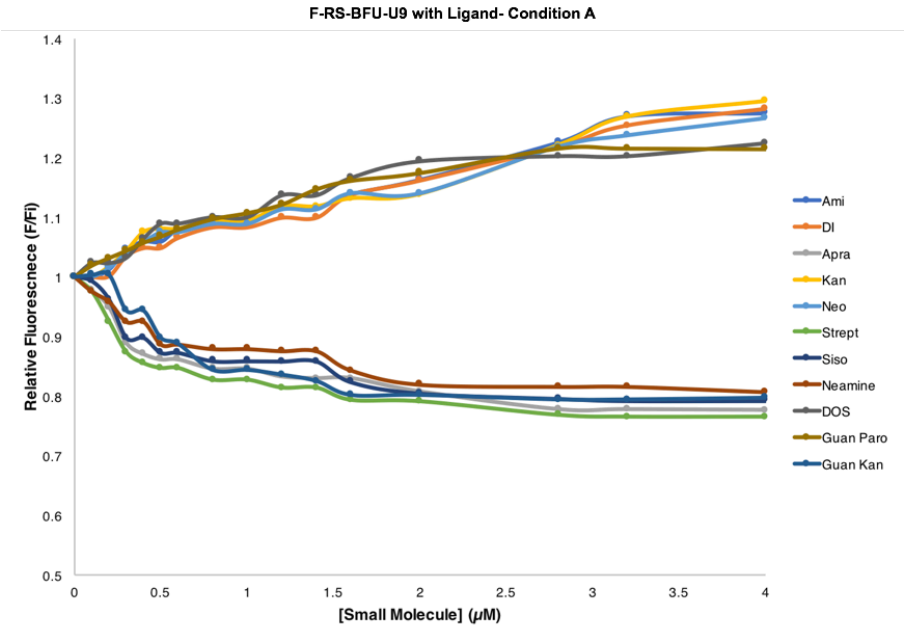
F-RS-BFU-U9 with Ligand- Condition A
Relative Fluorescnece (F/Fi)
[Small Molecule] (μM)
Ami
DI
Apra
Kan
Neo
Strept
Siso
Neamine
DOS
Guan Paro
Guan Kan

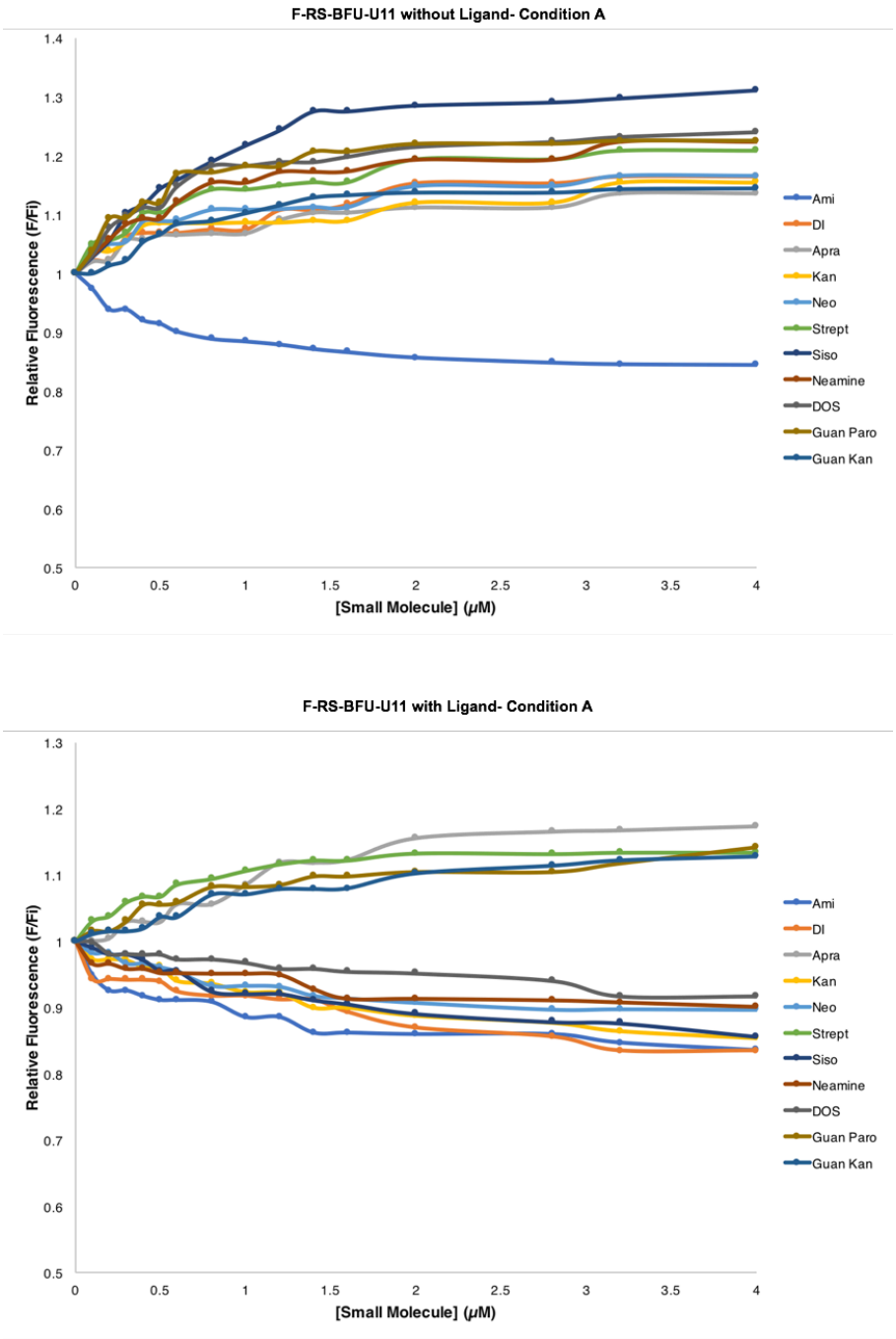

Figure S5-2. Fluoride riboswitch RNA constructs titration curves to the small molecule receptors in a standard buffer (10 mM NaH_2PO_4, 25 mM NaCl, 4 mM $MgCl_2$, 0.5 mM EDTA, pH 7.4) in the absence or presence of ligand (10 mM fluoride). Each graph shows a single RNA sequence and the receptors titration curves. The error for all experiments were less than 10%. The error was calculated using the standard error of triplicates, and relative standard error was determined based on the mean of each RNA sequence.

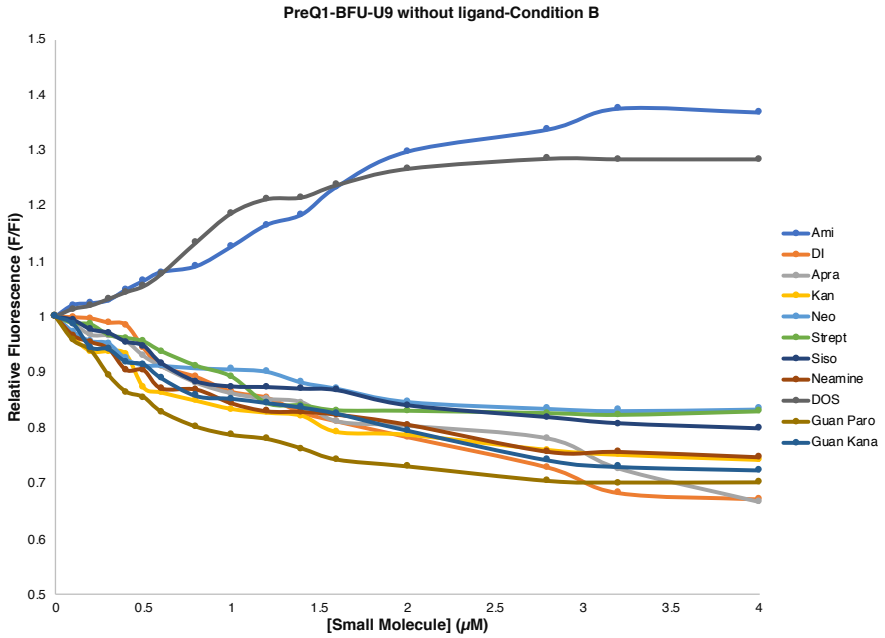
PreQ1-BFU-U9 without ligand-Condition B
Relative Fluorescence (F/Fi)
[Small Molecule] (μM)
Ami
DI
Apra
Kan
Neo
Strept
Siso
Neamine
DOS
Guan Paro
Guan Kana

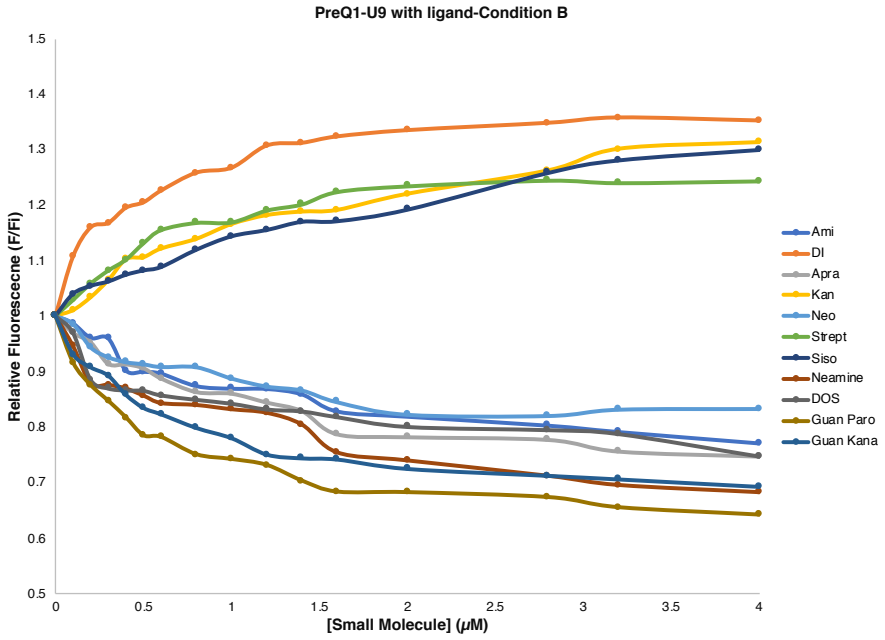
PreQ1-U9 with ligand-Condition B
Relative Fluorescecne (F/Fi)
[Small Molecule] (μM)
Ami
DI
Apra
Kan
Neo
Strept
Siso
Neamine
DOS
Guan Paro
Guan Kana

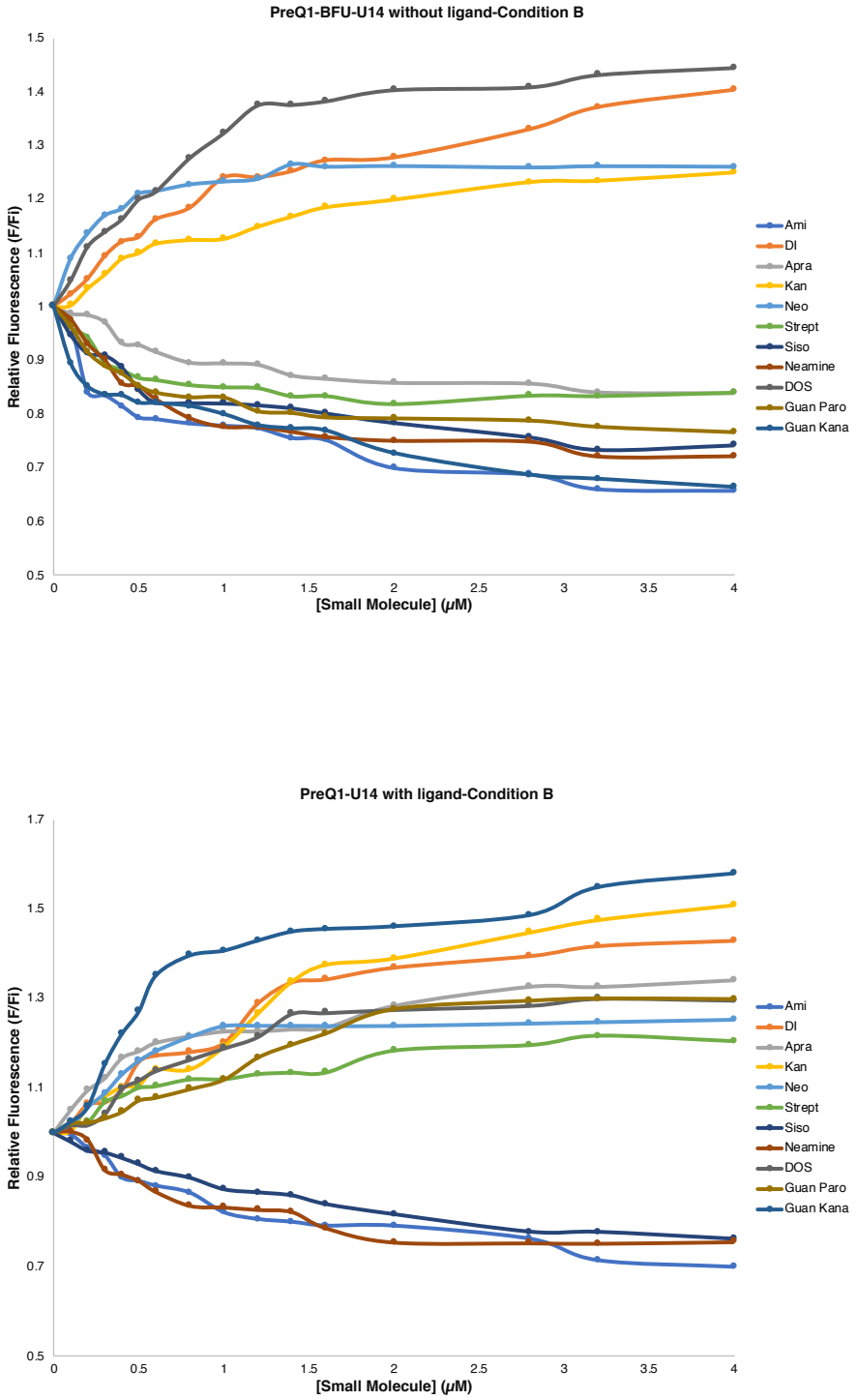

Figure S5-3. PreQ1 riboswitch RNA constructs titration curves to the small molecule receptors in a buffer with PEG at 37°C (10 mM NaH_2PO_4, 25 mM NaCl, 4 mM $MgCl_2$, 0.5 mM EDTA, 8 mM PEG 12,000, pH 7.4, 37°C) in the absence or presence of ligand (10 mM fluoride). Each graph shows a single RNA sequence and the receptors titration curves. The error for all experiments were less than 10%. The error was calculated using the standard error of

triplicates, and relative standard error was determined based on the mean of each RNA sequence.

S6. References

1. Eubanks, C. S.; Forte, J. E.; Kapral, G. J.; Hargrove, A. E., Small Molecule-Based Pattern Recognition To Classify RNA Structure. *J. Am. Chem. Soc.* **2017**, *139* (1), 409-416.
2. Eubanks, C. S.; Hargrove, A. E., Sensing the impact of environment on small molecule differentiation of RNA sequences. *Chem. Commun.* **2017**, *53* (100), 13363-13366.
3. Klepper, F.; Polborn, K.; Carell, T., Robust Synthesis and Crystal-Structure Analysis of 7-Cyano-7-deazaguanine (PreQ0 Base) and 7-(Aminomethyl)-7-deazaguanine (PreQ1 Base). *Helv. Chim. Acta* **2005**, *88* (10), 2610-2616.